Supplement of Atmos. Chem. Phys. Discuss., 14, 21565–21609, 2014
http://www.atmos-chem-phys-discuss.net/14/21565/2014/
doi:10.5194/acpd-14-21565-2014-supplement

Atmospheric Chemistry and Physics Discussions

Supplement of

Aqueous phase oligomerization of methyl vinyl ketone through photooxidation – Part 2: Development of the chemical mechanism and atmospheric implications

B. Ervens et al.

Correspondence to: B. Ervens (barbara.ervens@noaa.gov)

S1. Continuous-Flow EPR (electron paramagnetic resonance):

Transient radicals may be directly observed by mean of continuous-flow EPR. To use this technique for the present study, a steady state concentration of radicals was carried on the EPR cavity by pumping separated reactant solutions and mixing them prior the EPR cavity. The radicals were obtained using the following reactions:

$$Ti^{3+} + H_2O_2 \rightarrow Ti^{4+} + OH + OH^-$$

$$MVK + OH \rightarrow \text{Transient Radicals}$$

EPR experiments were carried out on a Bruker EMX instrument equipped with a TM4103 cylindrical cavity. Continuously degassed (Argon) aqueous solutions of MVK (25 mM (***Figure S1.1***) to 1 mM (***Figure S1.2***)) + H_2O_2 (25 to 10 mM, obtained from 30% H_2O_2 solution) and $Ti_2(SO_4)_3$ (2.5 mM (***Figure S1.1***) to 1 mM (***Figure S1.2***)obtained from a 20% aqueous solution in 1-4% sulfuric acid) were pumped by a 2 ways peristaltic pump (Cole-Parmer, typically 90 $mL.min^{-1}$/stream) and injected into a flow cell fitted within the EPR cavity. A mixing chamber located prior the cell allowed for simultaneous mixing of the two streams (the concentrations indicated previously are those obtained after mixing).

Comparing our experimental EPR spectra to simulations (***Figure S1***), the signal of $HO\text{-}CH_2\text{-}^{\bullet}CH\text{-}C(O)CH_3$ radical adduct resulting from pathway (1) was clearly distinguished. The radical species which proportion was concentration dependent (compare ***Figures S1.1 and S1.2***) was attributed to a dimer radical such as $HO\text{-}CH_2\text{-}CH(C(O)CH_3)\text{-}CH_2\text{-}^{\bullet}CH\text{-}C(O)CH_3$, thus confirming the very fast oligomerization pathway (Gilbert et al., 1994). However, more than two radical species were present in our experiments, but their respective signals remained unidentified due to overlapping EPR lines in the spectra.

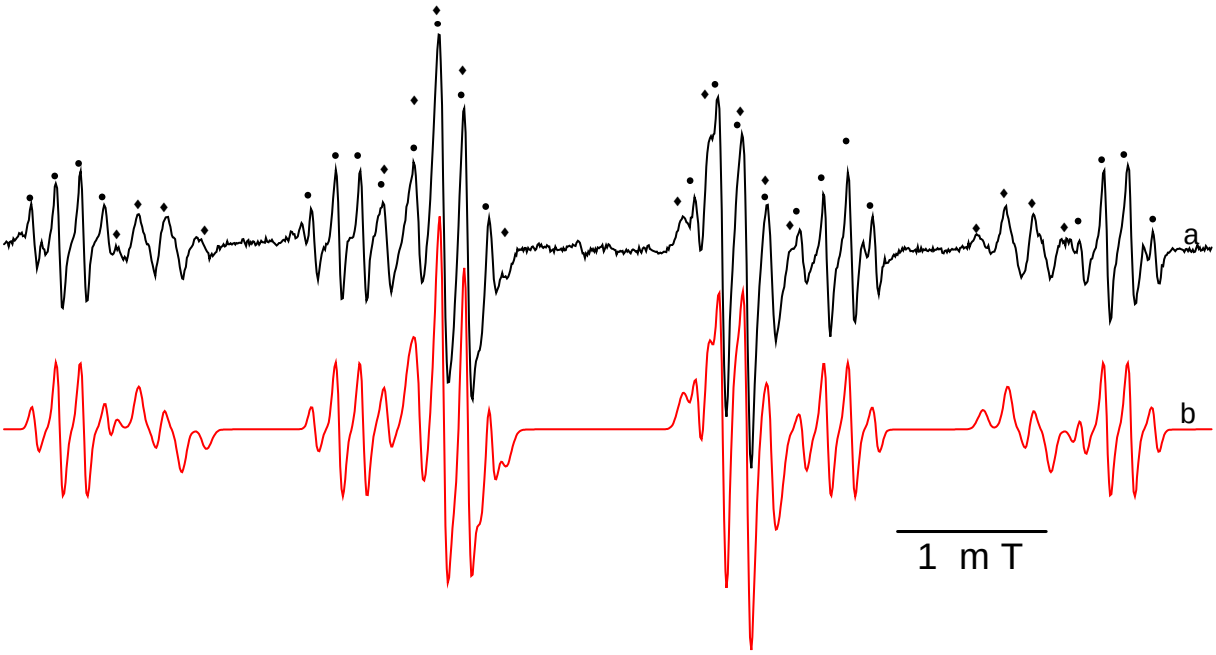

Figure S1.1: EPR spectra of radicals produced during reaction of hydroxyl radical with high initial concentrations of MVK (at pH = 1) : (**a**) experimental, (**b**) simulated. (•) HO-CH_2-·CH-C(O)CH_3 transient radicals (♦)HO-CH_2-C(H)(C(O)CH_3)-CH_2-·CH-C(O)CH_3 transient radicals. **[MVK] = 25 mM**, [Ti^{3+}] = 1.6 mM, [H_2O_2] = 16 mM, flow = 2x90 mL.min^{-1}. Setting : Power : 20 mW, Gain : 10^6, Scan Width 8.2 mT, Modulation Amplitude : 0.05 mT, Time Constant 81.9 ms, Scan Time : 1342.1 s.

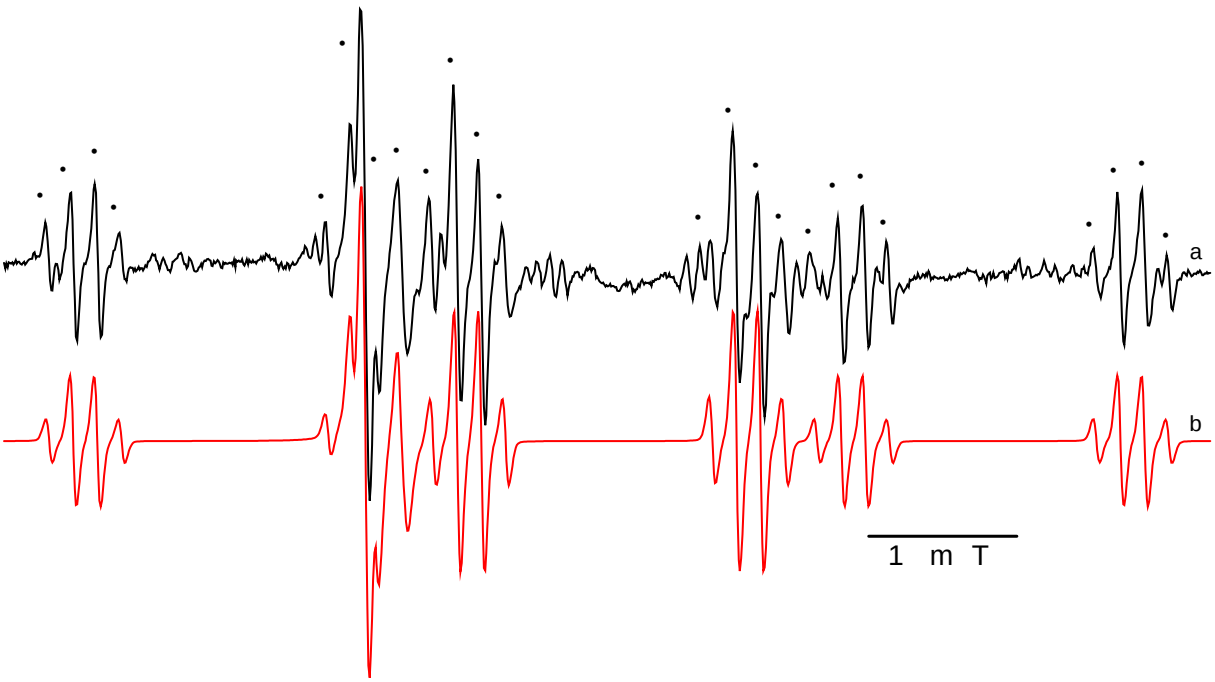

Figure S1.2: EPR spectra of radicals produced during reaction of hydroxyl radical with low initial concentrations of MVK (at pH = 1): (**a**) experimental, (**b**) simulated. (•) HO-CH_2-•CH-C(O)CH_3. **[MVK] = 1 mM**, [Ti^{3+}] = 1 mM, [H_2O_2] = 10 mM, flow = 2x90 mL.min^{-1}. Setting : Power : 20 mW, Gain : 10^6, Scan Width 8.2 mT, Modulation Amplitude : 0.05 mT, Time Constant 81.9 ms, Scan Time : 1342.1 s.

S2. Fits to measured O_2 concentration during experiments

The solutions of MVK, H_2O_2 and O_2 were continuously stirred during the experiments. The concentration of dissolved oxygen was highly variable with time and cannot be reproduced by the box model as described in Section 2.2.1. The oxygen concentration was continuously measured during the experiments by an oxymeter (Consort C3020). In order to constrain the oxygen concentrations in the simulations of the experiments, the measured oxygen concentrations were fitted, and the following fits were used as inputs to the model.

a) $[MVK]_0$ = 20 mM (Figure S1a):

$t < 780$ s Fit 1: $[O_2(aq)] = A - B \cdot t$

A = 531.71 ± 3.51
B = – 0.68523 ± 0.00774

$t \geq 780$ s Fit 2: $[O_2(aq)] = A + [B / [1 + \exp((C - t) / D)]]$

A = 7.1756 ± 0.121
B = 248.61 ± 0.943
C = 11734 ± 12.3
D = 1372.1 ± 7.14

b) $[MVK]_0$ = 5 mM (Figure S1b):

$t < 750$ s Fit 1: $[O_2(aq)] = A - B \cdot t$

A = 430.26 ± 3.27
B = -0.54381 ± 0.00662

$t \geq 750$ s Fit 2: $[O_2(aq)] = A + [B / [1 + \exp((C - t) / D)]]$

A = 13.799 ± 0.0415
B = 22.046 ± 1.92
C = 6958.6 ± 113
D = 669.98 ± 30.7

c) $[MVK]_0$ = 2 mM (Figure S1c):

$t < 1500$ s s Fit 1: $[O_2(aq)] = A + [B / [1 + \exp((C - t) / D)]]$

A = 395.8 ± 2.24
B = -385.09 ± 2.33
C = 236.6 ± 1.72
D = 111.36 ± 1.01

$t \geq 1500$ s Fit 2: $[O_2(aq)] = A + [B / [1 + \exp((C - t) / D)]]$

A = 5.5669 ± 0.319
B = 231.17 ± 1.48

C = 5536.2 ± 11.2
D = 965.2 ± 8.25

d) $[MVK]_0$ = 0.2 mM (Figure S1d):

t < 1000 s Fit 1: $[O_2(aq)] = A + B \cdot \exp(-C \cdot t)$

A = 160.17 ± 0.876
B = 130.6 ± 0.745
C = 0.0023561 ± 4.18e-005

t ≥ 1000 s Fit 2: $[O_2(aq)] = A - B \cdot t$

A = 145.64 ± 0.33
B = 0.024101 ± 0.000159

e) $[MVK]_0$ = 20 mM, low oxygen (Figure S1e):

$[O_2(aq)] = A + B * \exp(-C \cdot t) + D * \exp(-E \cdot t)$

A = 4.0001
B = 17.969
C = 0.3354
D = 37.411
E = 2.9862

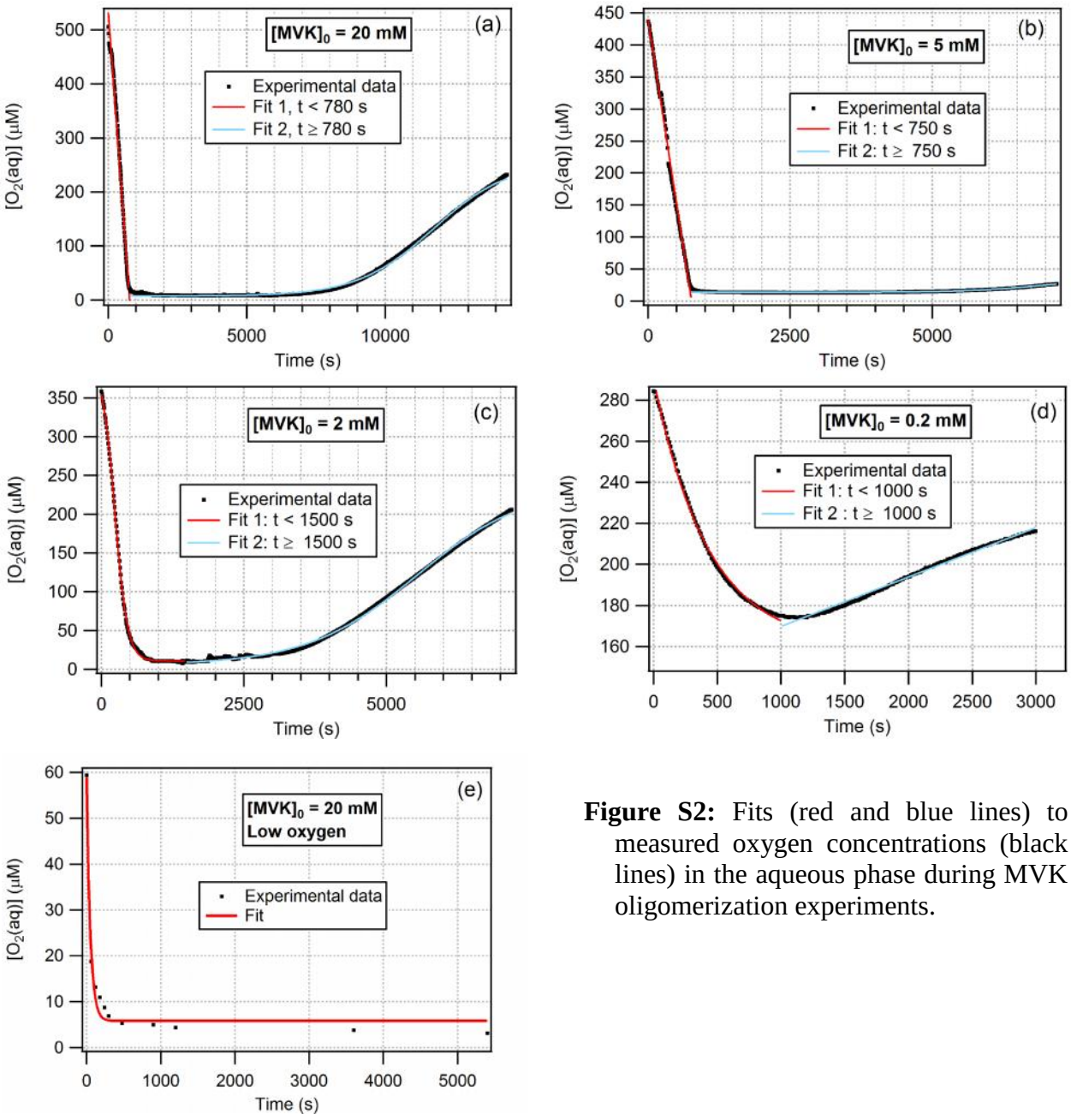

Figure S2: Fits (red and blue lines) to measured oxygen concentrations (black lines) in the aqueous phase during MVK oligomerization experiments.

S3. Fits to measured pH values during experiments

The initial pH value for all experiments was pH = 6. Due to the formation of organic acids (e.g. acetic acids or possibly acid functionalities on the oligomers), the pH value decreased to pH = 3 ($[MVK]_0 \geq 2$ mM), and to pH = 4 for $[MVK]_0 = 0.2$ mM) over the course of the experiment. For simplicity, we constrain the pH value by linear fits for the time scales shown in ***Figure 2***.

$pH = a - b \cdot t$ $\quad a = 6$

$[MVK]_0 = 20$ mM	b = 1/4800
$[MVK]_0 = 2$ mM and 5 mM	b = 1/2400
$[MVK]_0 = 0.2$ mM	b = 1/1500

S4. One-step representation of oligomerization

Based on additional laboratory studies, it can be assumed that MACR also forms oligomers by a similar mechanism as shown in ***Figure 1***. Since a detailed mechanism as for MVK is not available, we describe the oligomer formation rate by a simplified scheme

MVK or MACR + OH → Oligomers (R-S1)

with $k_{R\text{-}S1}$, chosen in a way that temporal evolution of the total oligomers in Figure 4 for all cases is approximated. It is obvious that none of the rate constants fits exactly all cases: ***Figure S3*** shows the comparison of oligomer evolution as predicted by the full mechanism in ***Figure 1 and Table 1*** and the predicted oligomer masses as predicted replacing the full mechanism by R-S1. Best agreement is found for a values within the range of 10^9 M^{-1} s^{-1} < $k_{R\text{-}3}$ < $1.5 \cdot 10^9$ M^{-1} s^{-1}, with a slightly higher value for the case using low initial oxygen concentrations ($k_{R\text{-}S1} = 2 \cdot 10^9$ M^{-1} s^{-1}). Based on this analysis, the simulations in Section 4 are performed with $k_{R\text{-}S1} = 1.5 \cdot 10^9$ M^{-1} s^{-1}.

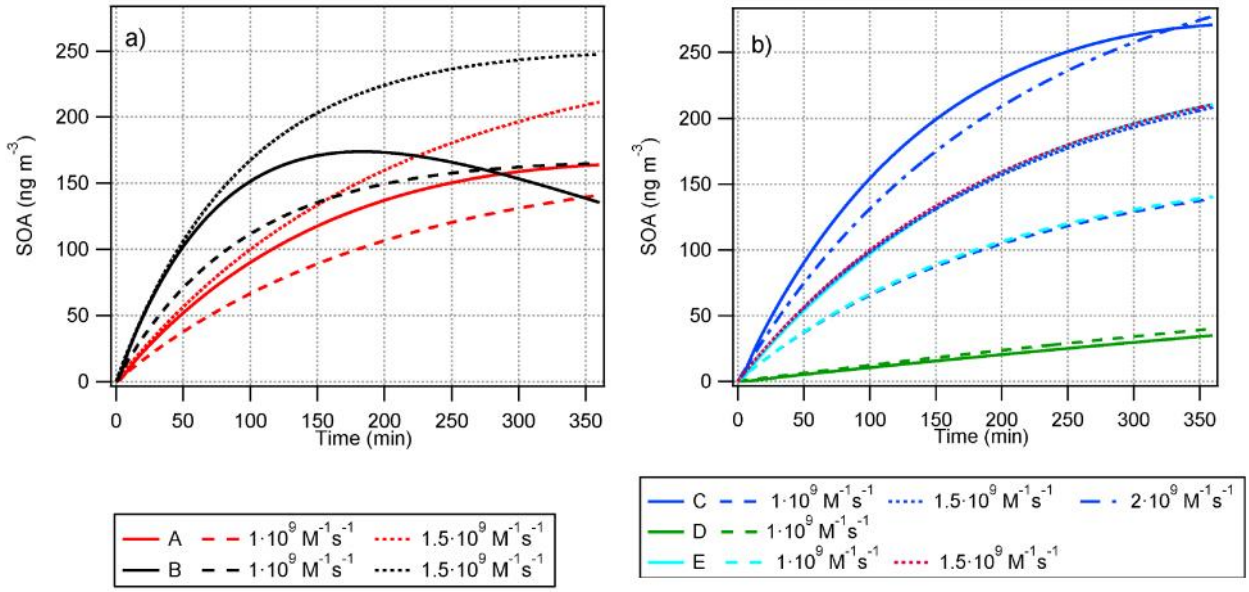

Figure S3: Predicted increase in oligomers in multiphase model (solid lines, these are the same results as in ***Figure 4***) and approximations for different $k_{R\text{-}S1}$ in order to represent oligomerization in a single step.